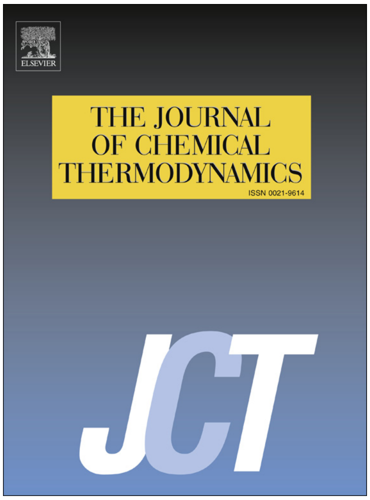

Solubilities of hydrofluorocarbons in ionic liquids: experimental and modelling study

José M.M.V. Sousa, José F.O. Granjo, António J. Queimada, Abel G.M. Ferreira, Nuno M.C. Oliveira, Isabel M.A. Fonseca

PII: S0021-9614(13)00254-1
DOI: http://dx.doi.org/10.1016/j.jct.2013.07.013
Reference: YJCHT 3605

To appear in: *J. Chem. Thermodynamics*

Please cite this article as: J.M.M. Sousa, J.F.O. Granjo, A.J. Queimada, A.G.M. Ferreira, N.M.C. Oliveira, I.M.A. Fonseca, Solubilities of hydrofluorocarbons in ionic liquids: experimental and modelling study, *J. Chem. Thermodynamics* (2013), doi: http://dx.doi.org/10.1016/j.jct.2013.07.013

This is a PDF file of an unedited manuscript that has been accepted for publication. As a service to our customers we are providing this early version of the manuscript. The manuscript will undergo copyediting, typesetting, and review of the resulting proof before it is published in its final form. Please note that during the production process errors may be discovered which could affect the content, and all legal disclaimers that apply to the journal pertain.

Solubilities of hydrofluorocarbons in ionic liquids: experimental and modelling study

José M.M.V. Sousa [a], *José F.O. Granjo* [b,*], *António J. Queimada* [1,c], *Abel G.M. Ferreira* [b], *Nuno M.C. Oliveira* [b], *Isabel M.A. Fonseca* [b]

[a]Department of Chemical and Biological Engineering, ISEC, Polytechnic Institute of Coimbra, Rua Pedro Nunes, Quinta da Nora, 3030-199 Coimbra, Portugal.

[b]Department of Chemical Engineering, University of Coimbra, Rua Sílvio Lima — Pólo II, 3030-790 Coimbra, Portugal

[c]Laboratory of Separation and Reaction Engineering (LSRE), Faculdade de Engenharia, Universidade do Porto, Rua do Dr. Roberto Frias, 4200-465 Porto, Portugal

*Corresponding author. Tel.: +351 239 798 793; Fax: + 351 239 798 703.

E-mail address: josegranjo@eq.uc.pt (José F.O. Granjo)

---

[1] Present address: Infochem Computer Services, 4, the Flag Store, 23 Queen Elizabeth Street, SE1 2LP London, UK.

ABSTRACT

In this work, experimental data on the gas solubility of hydrofluorocarbons (**CHF_3**, **CH_2F_2** and **CH_3F**) in four room-temperature ionic liquids (RTILs) were determined within the temperature range 288 K to 308 K and at atmospheric pressure. The RTILs used were 1-ethyl-3-methylimidazolium bis(trifluoromethanesulfonyl)imide(**[C_2mim][NTf_2]**), (trihexyl)tetradecyl-phosphoniumbis(trifluoro-methylsulfonyl)imide (**[$P_{6,6,6,14}$][NTf_2]**), and N-methyl-2-hydroxyethylammoniumpropionate (**[m-2-HEA][Pr]**) and pentanoate (**[m-2-HEA][P]**). Two modelling approaches, which we denote as predictive and correlative, were compared. In the former, the cubic plus association equation of state (CPA EoS) is used as a predictive model to estimate the solubilities using only pure components physical properties. In the latter, the regular-solution theory is the basis to build an empirical model whose parameters are obtained through least-squares fitting of experimental values.

Keywords:G/L solubility, Hydrofluorocarbon, Ionic liquid, CPA EoS, Regular Solution Model

1. Introduction

This study is a continuation of previous works [1, 2] where the solubility of some HFCs in volatile organic solvents (alcohols and aromatic solvents) was measured and correlated with the CPA EoS, to investigate the effect of association/solvation between solute and solvent molecules. Here, the solubility of CHF_3, CH_2F_2 and CH_3F in four RTILs ([C_2mim][NTf_2], [$P_{6,6,6,14}$][NTf_2],[m-2-HEA][Pr]and [m-2-HEA][P]) was determined as a function of temperature at atmospheric pressure, using a volumetric method with an automated apparatus [3].

The HFCs belong to an important class of compounds with industrial and household applications and they have been developed as alternative compounds due to the environmental concern of chlorofluorocarbons and hydrochlorofluorocarbons. Room temperature ionic liquids (RTILs) appear as a new type of solvents, in a class of substances belonging to molten salts with low melting points ($<$100 ºC) [4, 5] and non detectable vapour pressure. They are solely constituted by large organic cations like ammonium, imidazolium, phosphonium or pyridinium ions combined with organic or inorganic anions of smaller size and more symmetrical shape [6]. Their properties can be tuned by changing the ions according to the desired properties, from a very large set of possible combinations [7]. They possess numerous potential applications, replacing in some cases conventional volatile organic solvents while providing novel features in the application. Fundamental knowledge of the thermophysical properties of their mixtures with various chemicals is therefore critically important and needed, including the solubility of various compounds in ionic liquids (ILs). Due to the very large number of possible ILs, it is necessary to develop predictive and correlative models able to describe behaviours and properties based on experimental measurements of selected systems.

Yokozeki, Shiflett and co-workers have determined the solubility of various compounds such as HFCs in various RTILs [8-29]. They used a generic Redlich-Kwong type of cubic EoS [30], with a modified van der Waals-Berthelot mixing rule and critical properties of ILs estimated by Vetere's method [31]. Systems studied by this group include CO_2 in several different Ils [8-12], hydrofluorocarbons and hydrofluoroethers in some Ils [13-16], ammonia mixtures with Ils [17, 18], benzene and hexafluorobenzene in [C_2mim][NTf_2] [19], SO_2 in 1-butyl-3-methylimidazolium acetate ([C_4mim][Ac]) and1-butyl-3-methylimidazolium methylsulfate ([C_4mim][$MeSO_4$]) [20], water solubility in different Ils [21] and ternary systems with ILs, $CO_2$and H_2 [22], SO_2 [23], and H_2S [24, 25]. The authors present most of their results in graphical form and conclude that the model yields a good correlation of the experimental values. The same group later used a generic van der Waals EoS to model the solubility of gases CO_2, HFC-134a, SO_2 and NH_3in several imidazolium-based ILs [32]. Based on their results, as well as those in their previous studies, they conclude that all “cubic”' modified EoS work equally well for modelling PTx phase equilibria (solubility). In the present work, the observed solubility values are analyzed by a predictive model based on a cubic plus association equation of state (CPA EoS) to verify the accuracy of the CPA equation of state for description of the solubility data. The CPA EoS proposed by Kontogeorgis and co-workers [33] has been developed and applied to diverse systems since 1995, allowing a good description of phase behaviour with both associating and/or non-associating components. Later, a semi-empirical model based on the Regular Solution Theory (RST) is also adjusted to the experimental data. The goal of this modelling approach is to obtain a simple correlative model that can be readily used in process/product design.

2. Experimental

The experimental technique used in this work is based on a volumetric method. The apparatus used for the determination of solubility was described in detail elsewhere [3]. The principle of the apparatus is to bring an accurately known volume of solvent into contact with a known volume of gas at a given temperature and pressure. After the equilibrium is attained, the change in the gas volume yields the amount of gas dissolved in the liquid and hence the solubility. All RTILs and HFCs studied in this work are presented in table 1, along with their full names, abbreviations, chemical structures, origin and mass fraction purity for RTILs and % mol for HFCs. In order to decrease the water content and volatile compounds to negligible values all ILs were dried in vacuum (0.1 Pa) while stirring at moderate temperature (up to 60 ºC), for at least 24 h.

[Table 1 about here.]

3. Calculations and modelling

3.1. Gas solubility calculations

The procedure to estimate the mole fraction solubility of HFCs in RTILs (x_2) from experimental data is essentially similar to the ones adopted in earlier works [3, 34]. The amount in moles (n^G) and the volume of gas displaced due to dissolution (ΔV) can be related through a second-order truncated virial equation of state

$$\frac{PV_{mix}^G}{RT} = 1 + \frac{B_{mix}P}{RT} \tag{1}$$

where the molar volume of the gas mixture, V_{mix}^G, equals $\Delta V / n^G$, with n^G as the total amount of gas absorbed. P is the total pressure of gas; R is the universal gas constant; T is the temperature and B_{mix} is the second virial coefficient of the binary mixture:

$$B_{mix} = y_1^2 B_{11}(T) + y_2^2 B_{22}(T) + y_1 y_2 B_{12}(T) \tag{2}$$

Here y_1 and y_2 are the mole fraction composition in the vapour phase. The subscripts 1 and 2 represent the liquid solvent (RTIL) and the gas solute (HFC), respectively. $B_{11}(T)$, $B_{22}(T)$ and $B_{12}(T)$ are the second virial coefficients of pure components 1 and 2, and the second cross coefficient, respectively.

The calculations are simplified due to the extremely low vapour pressure of the RTILs (< 10 Pa), compared to the atmospheric pressure at which the experiences are performed and for the temperature range studied. Therefore, the RTILs are taken as strictly non-volatile solvents and consequently $y_2 \approx 1$, $B_{\text{mix}}(T) \approx B_{22}(T)$ and $n^G \approx n_2$. Rewriting Eq. 1 with the aforementioned simplifications, n_2 and $B_{22}(T)$ become:

$$n_2 = \Delta V / (RT / P + B_{22}(T)) \tag{3}$$

$$B_{22}(T) = \sum_{i=0}^{3} c_i T^{-i} \tag{4}$$

The parameters c_i of Eq. 4 for each HFC were retrieved from [35]. The solvent number of moles n_1, in turn, is evaluated from the difference of total solution mass m_s and the mass of solute $n_2 M_2$ at the end of each experiment:

$$n_1 = (m_s - n_2 M_2) / M_1 \tag{5}$$

Finally, x_2 is straight forwardly given by $x_2 = n_2 / (n_1 + n_2)$.

3.2. Gas solubility modelling

When the gas comes in contact with the liquid it dissolves partially in the latter. This process involves a change of enthalpy and entropy along with a decrease in gas volume until an equilibrium state is reached. In mathematical terms, the gas-liquid equilibrium condition for the solute can be expressed by a first-order condition (iso-fugacity) of Gibbs function, $f_2^G = f_2^L$. To model gas and liquid fugacities of HFCs (f_2^G and f_2^L, respectively) and calculate their solubility in RTILs, two strategies which we denote as predictive and correlative are employed.

In the former, a cubic-plus-association equation of state (CPA EoS) is used to model the equilibria. In this case, the solute solubilities are estimated using only solute and solvent pure physical properties. In this approach, the goal is to assess the capability of CPA EoS to be used as a tool for a more qualitative studies such as solvent screening. In the latter, the Regular Solution Theory (RST) provides theoretical background to build a semi-empirical model whose parameters are estimated through experimental data fitting. The objective here is to obtain simple mathematical expressions which can be readily used to predict solubilities. Both these approaches are described next.

3.2.1. CPA model

When an EoS is used, the liquid fugacity f_2^L is expressed by Eq. 6a and the gas fugacity f_2^G by Eq. 6b. To determine the fugacity coefficients of gas ϕ_2^G and liquid ϕ_2^L, the CPA EoS is applied.

$$f_2^L = x_2 \phi_2^L P \tag{6a}$$

$$f_2^G = \phi_2^G P \tag{6b}$$

The Cubic-Plus-Association (CPA) EoS proposed by Kontogeorgis *et al.* [36] can be expressed in terms of the compressibility factor Z which combines the simplicity of a cubic equation of state, the Soave-Redlich-Kwong (SRK EoS), that takes into account the physical interactions between the components, and an advanced associating term described by the Wertheim's theory, which accounts for the specific association parameters [37-39]:

$$Z = Z^{\text{phys.}} + Z^{\text{assoc.}} \tag{7a}$$

$$Z^{\text{phys.}} = \frac{1}{1-b\rho} - \frac{a\rho}{RT(1+b\rho)} \tag{7b}$$

$$Z^{\text{assoc.}} = -\frac{1}{2}\left(1+\rho\frac{\partial \ln g}{\partial \rho}\right)\sum_i x_i \sum_{A_i}(1-X_{A_i}) \tag{7c}$$

$$g(\rho) = \frac{1}{1-1.9\eta} \tag{7d}$$

$$\eta = \frac{1}{4}b\rho \tag{7e}$$

Here a, b and ρ are the energy parameter, co-volume parameter and the molar density, respectively; X_{A_i} represents the fraction of molecule i not bonded at site A, x_i is the mole fraction of component i and g the simplified radial distribution function [40]. The crucial point of the association term, X_{A_i}, is related with the association strength $\Delta^{A_iB_j}$ between sites belonging at different molecules, e.g. site A on molecule i and site B on molecule j, is defined as

$$X_{A_i} = \frac{1}{1+\rho\sum_j x_j \sum_{B_j} X_{B_j} \Delta^{A_iB_j}} \tag{8}$$

where the association strength, $\Delta^{A_iB_j}$, is expressed as:

$$\Delta^{A_iB_j} = g(\rho)\left[\exp\left(\frac{\varepsilon^{A_iB_j}}{RT}\right)-1\right] b_{ij}\beta^{A_iB_j} \tag{9}$$

The $\varepsilon^{A_iB_j}$ and $\beta^{A_iB_j}$ are the association energy and volume, respectively, while $b_{ij} = (b_i + b_j)/2$, where b_i is the temperature independent co-volume parameter of component i. For pure non-associating compounds, there are only three model parameters: the co-volume parameter b, and the parameters a_0 and c_1 in the Soave-type temperature dependency $a(T)$:

$$a(T) = a_0[1+c_1(1-T_r)]^2 \tag{10}$$

The model has two additional pure compound parameters for associating compounds, the $\varepsilon^{A_iB_j}$ and $\beta^{A_iB_j}$. These three or five parameters are typically obtained by fitting vapour pressure and liquid density data, carried by the minimization of an objective function:

$$\mathrm{OF} = \sum_i^{N_p}\left(\frac{P_i^{\mathrm{exp.}} - P_i^{\mathrm{calc.}}}{P_i^{\mathrm{exp.}}}\right)^2 + \sum_i^{N_p}\left(\frac{\rho_i^{\mathrm{exp.}} - \rho_i^{\mathrm{calc.}}}{\rho_i^{\mathrm{exp.}}}\right)^2 \tag{11}$$

When CPA is extended to mixtures, the energy and co-volume parameters of the physical term are calculated applying the conventional van der Waals one-fluid mixing rules:

$$a = \sum_i\sum_j x_i x_j a_{ij} \qquad \text{where} \quad a_{ij} = \sqrt{a_i a_j}(1-k_{ij}) \tag{12a}$$

$$b = \sum_i x_i b_i \tag{12b}$$

When dealing with mixtures containing associating molecules, the association term of the CPA EoS, requires combining rules for the association energy and volume parameters [33], in order to calculate the value of the association strength in Eq. 9. Over the last years various combining rules have been investigated [41, 42]. The Elliott combination rule is used in the present work:

$$\Delta^{A_iB_j} = \sqrt{\Delta^{A_iB_i}\Delta^{A_jB_j}} \tag{13}$$

To account for solvation, Folas *et al.* [43] suggested the modified CR-1 rule (mCR-1):

$$\varepsilon^{A_iB_j} = \frac{\varepsilon_{\text{associating}}}{2} \qquad \text{and} \qquad \beta^{A_iB_j} = \beta_{\text{cross}} \equiv \text{fitted} \tag{14}$$

3.2.2. A RST-based correlative model

The RST was developed to model solutions that behave almost as regular solutions, *i.e.*, have vanishing excess entropy and excess volume of mixing at constant temperature and pressure. In these cases, the isothermal dissolution of a gas can be conceptualized as a two-step process. First the gas "condenses" to its partial volume in the liquid solvent 1 with its partial Gibbs energy. Hence $\overline{g}_2 = RT\ln f_2^{o,L}$, where $f_2^{o,L}$ is the solute fugacity at its standard state, *i.e.*, pure "liquid 2" at equilibrium conditions. The second step is the dissolution of pure "liquid 2" in solvent 1 where its partial Gibbs energy is given by $\overline{g}_2 = RT\ln\gamma_2 x_2$, where γ_2 is the solute activity coefficient with pure "liquid 2" as the standard state [44]. Following this reasoning, the solute liquid fugacity is expressed by:

$$f_2^L = x_2\gamma_2 f_2^{o,L} \tag{15}$$

If the Scatchard-Hildebrand equation is applied for γ_2:

$$\begin{gathered}\ln\gamma_2 = V_{m,2}^L\Phi_1^2(\delta_1-\delta_2)^2/(RT) \approx V_{m,2}^L(\delta_1-\delta_2)^2/(RT)\\ \text{as } \Phi_1^2 \approx 1 \text{ with } x_2 << 1\end{gathered} \tag{16}$$

Eq. 16 shows that the RST model always predicts positive deviations to Raoult's law ($\gamma_2 \geq 1$), and γ_2 is mainly function of both solvent and solute solubility parameters (δ_1 and δ_2, respectively).The $V_{m,2}^L$ represents solute's liquid molar volume and Φ_1 solvent's volume fraction.

Although originally RST was conceived for non-electrolytes solutions, it has been applied with success to estimate the solubility of simple gases in Ils [45-49]. As pointed out by Scovazzo *et al.* [46], the electrolyte character of the solutions containing ILs is dependent whether the Coulombic or van der Waals forces are predominant. In this work, it is assumed that short-range forces dominate and this hypothesis will be tested by assessing whether the RST model can explain the relative solubility of HFCs in RTILs.

Manipulating Eq. 15 we define the Henry's constant of the gas H_{21} as:

$$H_{21} \equiv \frac{f_2^L}{x_2} = \frac{f_2^G}{x_2} \tag{17}$$

It must be noted that H_{21} above differs from the classical definition of Henry's constant $H_{21} \equiv \lim_{x_2 \to 0} (f_2^L / x_2)$, where for a binary mixture it depends on the temperature and pressure but not on the mole fraction [50, chap. 10]. Combining Eq. 16 and 17 and assuming that the entropic or combinatorial effects are approximately constant for a specific gas, we obtain:

$$\ln H_{21} = \frac{V_{m,2}^L (\delta_1 - \delta_2)^2}{RT} + \ln f_2^{o,L} \approx D + \frac{E(\delta_1 - \delta_2)^2}{T} \tag{18}$$

The parameters D and E are only function of the solute and are estimated from a least-squares fit of $\ln H_{21}$ versus $(\delta_1 - \delta_2)^2 / T_{\text{ref}}$ data, for a given reference temperature T_{ref}.

The experimental values for δ_2 are listed in table 2. The values for δ_1's are estimated using a similar approach as the one described in Camper *et al.* [47]. They assume that the lattice structures of RTILs share similarities with the molten salts and then use the results of Takamatsu [51] to estimate δ_1:

$$\delta_1 = (\frac{U_1}{V_{m,1}^L})^{1/2} \tag{19a}$$

$$U_1 = 1.2025\times10^{-2}\cdot\left(\frac{\nu\cdot|z_c z_a|}{r_c + r_a}\right)\left(1-\frac{3.45\times10^{-9}}{r_c + r_a}\right) \tag{19b}$$

$$V_{m,1}^{L} = 2N_{av}(r_c + r_a)^3 \tag{19c}$$

Since the Coulombic forces are the stronger forces inside RTILs, the lattice energy density U_1 /(J·mol^{-1}) is used to estimate δ_1 , instead of the energy of vaporization. The U_1 is calculated using the Kapustinskii's equation where Z_a and Z_c are, respectively, the valency of anion and cation which have unitary value for all RTILs in this study; ν is the number of ions in the chemical formula and its value is two also for all RTILs; r_a and r_c are, respectively, the radii of anion and cation (calculated from Eq. 19c). The liquid molar volume of RTILs, $V_{m,1}^{L}$ /(cm^3·mol^{-1}), was estimated using correlations obtained from experimental data published in open literature and can be consulted in the supplementary data materials. In section 4.3 the values of the solubility parameters δ_1 for RTILs and the parameters D and E for the semi-empirical model of Eq. 18 are presented and discussed for each binary system studied. The gas fugacity coefficient (ϕ_2^G) in Eq. 6b is now calculated using a virial equation of state:

$$\ln\phi_2^G = \frac{B_{22}(T)P}{RT} \tag{20}$$

[Table 2 about here.]

4. Results and discussion

4.1. Experimental results

Table 3 shows the solubility data and the Henry's constants for HFCs in RTILs solvents, for several temperatures at 0.101 MPa. Full experimental data can be found in the supporting information materials. The results show that for each HFC the solubilities increase in the order [m-2-HEA][Pr]< [m-2-HEA][P] < [C_2mim][NTf_2] < [$P_{6,6,6,14}$][NTf_2], and among RTILs the solubilities increase in the order CHF_3< CH_3F < CH_2F_2. The HFCs are more soluble in [C_2mim][NTf_2] and [$P_{6,6,6,14}$][NTf_2] (up to roughly 2.5 times more than in ammonium-based RTILs). The differences in the HFC solubilities in $[C_2mim][NTf_2]$ and $[P_{6,6,6,14}][NTf_2]$ are explained by the size of the cation of each RTIL, which increases the free volume in the RTIL. However, a large difference among the solubility values was expected, since the size of $[P_{6,6,6,14}]$ cation is significantly larger than the $[C_2mim]$ cation. This may indicate that the $[NTf_2]$ anion of these RTILs also plays a significant role in the solubility. Indeed Shiflett *et al.* [26] found large solubility differences between ionic liquids with fluorinated anions (higher solubility for CH_2F_2) and non-fluorinated anions (lower solubility for CH_2F_2), suggesting that at the intermolecular level the hydrogen bond (H···F) plays an important role between the hydrogen atoms in the HFCs and the multiple anion fluorines, as well as the fluorines of the HFCs and the multiple cation hydrogen atoms. The lower solubility values of HFCs in ammonium based RTILs compared to the $[C_2mim][NTf_2]$ and $[P_{6,6,6,14}][NTf_2]$ RTILs can be related with the size of the RTILs, although strong hydrogen bonds (H···O) of the propionate and pentanoate anions with the [m-2-HEA] cation can also contribute to this fact, making the anion less available for interaction with HFCs. Comparing the present values of the solubility of HFCs with those in other solvents studied in previous works at 0.101 MPa [1, 2], we find that the solubilities of CHF_3in $[C_2mim][NTf_2]$ are comparable to the values in the lower alcohols, while the solubilities in ammonium based ILs are closer to the values found in aromatic solvents. For CH_2F_2, the solubilities in ammonium based RTILs are slightly higher than those in lower alcohols and aromatic solvents. Finally, for CH_3F it was found that the solubilities in lower alcohols were lower than both in aromatic and ammonium based RTILs solvents.

[Table 3 about here.]

4.2. CPA EoS model

The HFCs studied in this paper were treated as non-associating compounds, while the ILs were treated as non-associating and also as association compounds with a two-site (2B) scheme. Parameters for the pure component CPA were proposed in Sousa *et al.* [2] for HFCs, Maia *et al.* [52] $[C_2mim][NTf_2]$ and Manic *et al.* [53] for $[P_{6,6,6,14}][NTf_2]$. To calculate the CPA pure parameters for [m-2-HEA][Pr]; and [m-2-HEA][P], liquid density data for these ILs were obtained in the literature [54]. As no vapour pressure data could be found for these ammonium ILs, it was assumed that in the reduced temperature range between 0.40 and 0.60, the vapour pressures could be described by the equation $\ln P = A - B / T$, where the A and B parameters were regressed considering a vapour pressure of 10^{-6} Pa at T = 273.15 K and the critical pressure. The critical properties and acentric factors were obtained from Valderrama *et al.*, estimated applying the modified Lydersen-Joback-Reid method [55, 56]. The pure compound parameters for the studied HFCs and ILs are reported in Table 4 along with the absolute average deviations (AAD) calculated for vapour pressures P^{σ} and molar densities $\rho_{\text{liq.}}$ after minimization of Eq. 11.

[Table 4 about here.]

Prediction of the HFCs solubilities in the ILs was carried out using the estimated pure component parameters in the CPA EoS, without the k_{ij} binary interaction parameters (prediction), considering two schemes for the ILs: NA (non-associating) and the 2B (two-association sites).

[Table 5 about here.]

Tables 4 and 5 show that there is no clear advantage in considering association in the ILs for describing either their pure component properties or the HFCs solubilities in the presented (HFCs + ILs) systems. Table 5 and figures 1 to 3 also show that the CPA EoS describes in the correct order the HFC solubilities in RTILs.

[Figure 1 about here.]

[Figure 2 about here.]

[Figure 3 about here.]

4.3. RST-based model

The solubility parameters δ_1 calculated from Eqs. 19 and listed in table 6 vary from (19.4 to 57.2)

$(\mathrm{J \cdot cm^{-3}})^{1/2}$ for $[\mathrm{P}_{6,6,6,14}][\mathrm{NTf}_2]$ and [m-2-HEA][Pr], respectively. The δ_1 values reported here are within the expected range and are consistent with Camper *et al.* [47], where solubility parameters were estimated for other RTILs and then compared with common solvents. The δ_1 of $[\mathrm{P}_{6,6,6,14}][\mathrm{NTf}_2]$ is closer to the solubility parameters of aromatics, as a consequence of the weak ionic interactions, due to the larger size of its ions. For $[\mathrm{C_2mim}][\mathrm{NTf}_2]$, [m-2-HEA][Pr] and [m-2-HEA][P], the δ_1 values are greater than lower alcohols and closer to simple organic salts, since the ionic interactions are stronger than the polar interactions.

[Table 6 about here.]

Figures 4 to 6 show the variation of $\ln H_{21}$ against $(\delta_1 - \delta_2)^2 / T$. As can be observed, the HFC solubilities increase with the decrease of $(\delta_1 - \delta_2)^2$, showing a qualitative agreement with the thumb rule "like dissolves like", *i.e.*, solutes with cohesive energies closer to solvents' tend to dissolve to greater extent. However, this conclusion cannot be extrapolated to other solvents, like alcohols or aromatics [1, 2], since chemical effects resulting from the electrophilic nature of HFCs or from the polarization degree of the solvents may have far more impact in the solubilities than only the cohesive energies of both HFC and solvent.

[Figure 4 about here.]

[Figure 5 about here.]

[Figure 6 about here.]

Table 7 lists the parameters of Eq. 18 obtained after least-squares fitting. Significant errors are observed when predicting the influence of temperature in HFC solubilities. This results from the fact that as temperature increases, Eq. 18 predicts an increasing in the solubilities while experimentally the opposite behaviour is observed. Therefore, while the RST model is able to predict the relative solubility among solvents, it fails to describe the solubilities change with temperature.

[Table 7 about here.]

To overcome this limitation of the RST model, γ_2 in Eq. 15 is partitioned in two parts (Eq. 21): a residual part (γ_2^{res}) that represents the enthalpic effects (Scatchard-Hildebrand equation in the form of Eq. 18), and a combinatorial part ($\gamma_2^{*,comb}$) which accounts for the entropic effects. For the latter, the two-suffix Margules equation was chosen (Eq. 22). Despite its simple nature, it provides a comparable description as other more complex one-parameter local composition-based models such one-parameter NRTL described in Vetere [57]:

$$\gamma_2 = \gamma_2^{*,\mathrm{comb}} \gamma_2^{\mathrm{res}} \tag{21}$$

$$\ln \gamma_2^{*,\mathrm{comb}} = \frac{A x_1^2}{R}(1/T - 1/T_{\mathrm{ref}}) \tag{22}$$

$\gamma_2^{*,\mathrm{comb}}$ is the activity coefficient of the combinatorial part normalized to the temperature of reference (T_{ref}= 288.15 K). The Margules parameter (A/R) values are listed in table 8. Results show now a good quantitative agreement between experimental and predicted solubilities. In figures 1 to 3 in the previous section 4.2, the solubilities predicted are plotted against experimental solubilities together with CPA EoS predictions.

5. Conclusions

This paper reports data on the solubility of HFCs (CHF_3, CH_2F_2 and CH_3F) in four RTIL solvents ([C$_2$mim][NTf$_2$]; [P$_{6,6,6,14}$][NTf$_2$] ; [m-2-HEA][Pr] and [m-2-HEA][P]) determined within the temperature range between 288 K to 308 K at 0.101 MPa. It was found that among the solvents, the solubilities were greater in [P$_{6,6,6,14}$][NTf$_2$] while lower in the ammonium cation based RTILs. Data were then modelled using two approaches named as predictive and correlative.

In the first, the CPA EoS was applied for the prediction (without k_{ij} binary interaction parameters) of HFCs solubilities in ionic liquids. According to the results, CPA EoS was able to predict in a qualitative way the solubilities between HFC-RTIL systems, by predicting the relative solubility of

HFC in IL in the correct order. Therefore, the CPA EoS can be a useful tool to screen other ILs of interest to dissolve HFCs. Also we conclude that there is no clear advantage in considering association in the ionic liquids for describing either their pure component properties or the HFCs solubilities in the presented ILs systems.

In the second approach, a semi-empirical model based on RST was adjusted to experimental data. Results show that, although this model fails to predict the influence of the temperature in solubilities, it predicts the relative solubilities between HFC-RTIL systems at a given reference temperature (288.15 K). It was also found that solubilities increased as the difference square between solubility parameters of HFC and RTIL decreases. Although this conclusion is in agreement with previous works [45, 47], it does not hold for other common solvents, like aromatic and lower alcohols studied in previous works [1, 2]. Later in this approach, a combinatorial term in a Margules-like form, was introduced in the initial RST-based model to account for entropic effects. The resulting model gave a better quantitative description of the experimental data with AAD(x_2) values around 5 %.

Acknowledgments

The authors acknowledge financial support provided by Fundação para a Ciência e Tecnologia (Portugal) through the Ph.D. grant SFRH/BD/64338/2009 of J.F. Granjo and the Ph.D. grant SFRH/PROTEC/67482/2010 of J.M.M.V. Sousa. Authors would like to thank to Professor J.A.P. Coutinho for [m-2-HEA][Pr] and [m-2-HEA][P] ionic liquids.

References

[1] J. Sousa, J. Almeida, A. Ferreira, H. Fachada, I. Fonseca, Fluid Phase Equilibria 303 (2011) 115–119.

[2] J. Sousa, A. Queimada, E. Macedo, I. Fonseca, Fluid Phase Equilibria 337 (2013) 60–66.

[3] I. Fonseca, J. Almeida, H. Fachada, The Journal of Chemical Thermodynamics 39 (2007) 1407–1411.

[4] P. Wasserscheid, T. Welton (Eds.), Ionic Liquids in Synthesis, Second Edition, 2008.

[5] K. R. Seddon, Journal of Chemical Technology & Biotechnology 68 (1997) 351–356.

[6] A. Heintz, The Journal of Chemical Thermodynamics 37 (2005) 525–535.

[7] J. D. Holbrey, K. R. Seddon, Clean Products and Processes 1 (1999) 223–236.

[8] M. B. Shiflett, A. Yokozeki, Industrial & Engineering Chemistry Research 44 (2005) 4453–4464.

[9] M. B. Shiflett, A. Yokozeki, The Journal of Physical Chemistry B 111 (2007) 2070–2074.

[10] M. B. Shiflett, D. J. Kasprzak, C. P. Junk, A. Yokozeki, The Journal of Chemical Thermodynamics 40 (2008) 25–31.

[11] A. Yokozeki, M. B. Shiflett, C. P. Junk, L. M. Grieco, T. Foo, The Journal of Physical Chemistry B 112 (2008) 16654–16663.

[12] M. B. Shiflett, A. Yokozeki, Journal of Chemical & Engineering Data 54 (2009) 108–114.

[13] M. B. Shiflett, A. Yokozeki, Journal of Chemical & Engineering Data 51 (2006) 1931–1939.

[14] A. Yokozeki, M. B. Shiflett, AIChE Journal 52 (2006) 3952–3957.

[15] M. B. Shiflett, A. Yokozeki, Journal of Chemical & Engineering Data 53 (2008) 492–497.

[16] J. Kumelan, A. Perez-Salado Kamps, D. Tuma, A. Yokozeki, M. B. Shiflett, G. Maurer, The Journal of Physical Chemistry B 112 (2008) 3040–3047.

[17] A. Yokozeki, M. B. Shiflett, Industrial & Engineering Chemistry Research 46 (2007) 1605–1610.

[18] A. Yokozeki, M. B. Shiflett, Applied Energy 84 (2007) 1258–1273.

[19] A. Yokozeki, M. B. Shiflett, Industrial & Engineering Chemistry Research 47 (2008) 8389–8395.

[20] M. B. Shiflett, A. Yokozeki, Industrial & Engineering Chemistry Research 49 (2010) 1370–1377.

[21] A. Yokozeki, M. B. Shiflett, Industrial & Engineering Chemistry Research 49 (2010) 9496–9503.

[22] A. Yokozeki, M. B. Shiflett, Applied Energy 84 (2007) 351–361.

[23] M. B. Shiflett, A. Yokozeki, Energy & Fuels 24 (2010) 1001–1008.

[24] M. B. Shiflett, A. Yokozeki, Fluid Phase Equilibria 294 (2010) 105–113.

[25] M. B. Shiflett, A. M. S. Niehaus, A. Yokozeki, Journal of Chemical & Engineering Data 55 (2010) 4785–4793.

[26] M. B. Shiflett, M. A. Harmer, C. P. Junk, A. Yokozeki, Journal of Chemical & Engineering Data 51 (2006) 483–495.

[27] M. B. Shiflett, A. Yokozeki, AIChE Journal 52 (2006) 1205–1219.

[28] M. B. Shiflett, M. A. Harmer, C. P. Junk, A. Yokozeki, Fluid Phase Equilibria 242 (2006) 220–232.

[29] M. B. Shiflett, A. Yokozeki, Industrial & Engineering Chemistry Research 45 (2006) 6375–6382.

[30] A. Yokozeki, International Journal of Thermophysics 22 (2001) 1057–1071.

[31] A. Vetere, The Chemical Engineering Journal 49 (1992) 27–33.

[32] A. Yokozeki, M. B. Shiflett, The Journal of Supercritical Fluids 55 (2010) 846–851.

[33] G. M. Kontogeorgis, M. L. Michelsen, G. K. Folas, S. Derawi, N. Von Solms, E. H. Stenby,

Industrial & Engineering Chemistry Research 45 (2006) 4855–4868.

[34] P. Husson-Borg, V. Majer, M. F. Costa Gomes, Journal of Chemical & Engineering Data 48 (2003) 480–485.

[35] J. H. Dymond, K. N. Marsh, R. C. Wilhoit, K. C. Wong, in: M. Frenkel, K. N. Marsh (Eds.), Virial Coefficients of Pure Gases, number 21A in Landolt-B rnstein - Group IV Physical Chemistry, Springer Berlin Heidelberg, 2002, pp. 83–109.

[36] G. M. Kontogeorgis, E. C. Voutsas, I. V. Yakoumis, D. P. Tassios, Industrial & Engineering Chemistry Research 35 (1996) 4310–4318.

[37] M. L. Michelsen, E. M. Hendriks, Fluid Phase Equilibria 180 (2001)165–174.

[38] J. Wu, J. M. Prausnitz, Industrial & Engineering Chemistry Research37 (1998) 1634–1643.

[39] E. C. Voutsas, G. C. Boulougouris, I. G. Economou, D. P. Tassios,Industrial & Engineering Chemistry Research 39 (2000) 797–804.

[40] G. M. Kontogeorgis, I. V. Yakoumis, H. Meijer, E. Hendriks, T. Moorwood, Fluid Phase Equilibria 158–160 (1999) 201–209.

[41] S. O. Derawi, G. M. Kontogeorgis, M. L. Michelsen, E. H. Stenby, Industrial & Engineering Chemistry Research 42 (2003) 1470–1477.

[42] E. C. Voutsas, I. V. Yakoumis, D. P. Tassios, Fluid Phase Equilibria158–160 (1999) 151–163.

[43] G. K. Folas, G. M. Kontogeorgis, M. L. Michelsen, E. H. Stenby, Industrial & Engineering Chemistry Research 45 (2006) 1516–1526.

[44] J. H. Hildebrand, J. M. Prausnitz, R. L. Scott, Regular and related solutions: the solubility of gases, liquids, and solids, Van NostrandReinholdCo., 1970.

[45] D. Camper, P. Scovazzo, C. Koval, R. Noble, Industrial & EngineeringChemistry Research 43 (2004) 3049–3054.

[46] P. Scovazzo, D. Camper, J. Kieft, J. Poshusta, C. Koval, R. Noble,Industrial & Engineering Chemistry Research 43 (2004) 6855–6860.

[47] D. Camper, C. Becker, C. Koval, R. Noble, Industrial & EngineeringChemistry Research 44 (2005) 1928–1933.

[48] A. Finotello, J. E. Bara, S. Narayan, D. Camper, R. D. Noble, TheJournal of Physical Chemistry B 112 (2008) 2335–2339.

[49] A. Finotello, J. E. Bara, D. Camper, R. D. Noble, Industrial & Engineering Chemistry Research 47 (2008) 3453–3459.

[50] J. M. Prausnitz, R. N. Lichtenthaler, E. G. d. Azevedo, Molecular Thermodynamics of FluidPhase Equilibria, Prentice Hall, 1998.

[51] T. Takamatsu, Bulletin of the Chemical Society of Japan 47 (1974)1287–1288.

[52] F. M. Maia, I. Tsivintzelis, O. Rodriguez, E. A. Macedo, G. M. Kontogeorgis, Fluid Phase Equilibria 332 (2012) 128–143.

[53] M. S. Manic, A. J. Queimada, E. A. Macedo, V. Najdanovic-Visak, TheJournal of Supercritical Fluids 65 (2012) 1–10.

[54] N. M. Talavera-Prieto, A. G. M. Ferreira, P. N. Sim es, P. J. Carvalho, J. A. Coutinho, Pressure-volume-temperature and calorimetric measurements of ammonium protic ionic liquids, 2013. Unpublished.

[55] J. O. Valderrama, P. A. Robles, Industrial & Engineering ChemistryResearch 46 (2007) 1338–1344.

[56] J. O. Valderrama, W. W. Sanga, J. A. Lazzus, Industrial & EngineeringChemistry Research 47 (2008) 1318–1330.

[57] A. Vetere, Fluid Phase Equilibria 218 (2004) 33–39.

[58] V. H. Álvarez, N. Dosil, R. Gonzalez-Cabaleiro, S. Mattedi, M. Martin-Pastor, M. Iglesias, J. M. Navaza, Journal of Chemical & EngineeringData 55 (2010) 625–632.

[59] C. Yaws, Chemical Properties Handbook, McGraw-Hill, 1999.

List of Figures

Figure 1. Plot of calculated values of solubilit $x_2(\text{calc.})$ using the predictive model in Eqs. (7) and (17) (○□◇△) and the correlative model of Eqs. (17), (21) and (22) (●■◆▲) against experimental solubility $x_2(\text{exp.})$ for CHF_3 in RTILs.

Figure 2. Plot of calculated values of solubility $x_2(\text{calc.})$ using the predictive model in Eqs. (7) and (17) (○□◇△) and the correlative model of Eqs. (17), (21) and (22) (●■◆▲) against experimental solubility $x_2(\text{exp.})$ for CH_2F_2 in RTILs.

Figure 3. Plot of calculated values of solubility $x_2(\text{calc.})$ using the predictive model in Eqs. (7) and (17) (○□◇△) and the correlative model of Eqs. (17), (21) and (22) (●■◆▲) against experimental solubility $x_2(\text{exp.})$ for CH_3F in RTILs.

Figure 4. Plof of the logarithm of Henry's constants for CHF_3 in RTILs versus the squared of the difference between solubility parameters of solvents (1) and solute (2) at reference temperature T_{ref} of (288.15 ± 0.01) K.

Figure 5. Plot of the logarithm of Henry's constant for CH_2F_2 in RTILs versus the squared of the difference between solubility parameters of solvents (1) and solute (2) at reference temperature T_{ref} of (288.15 ± 0.01) K.

Figure 6. Plot of the logarithm of Henry's constant for CH_3F in RTILs versus the squared of the difference between solubility parameters of solvents (1) and solute (2) at reference temperature T_{ref} of (288.15 ± 0.01) K.

List of Tables

Table 1. Compounds used in this work.

Table 2.HFC solubility parameters δ_2 at the boiling point temperature. Values retrieved from [59].

Table 3. Experimental solubilities x_2 and Henry's constants H_{21} for CHF_3, CH_2F_2 and CH_3F in RTILs at).101 MPa as a function of temperature.

Table 4. Pure component CPA parameters a_0, c_1, b and β Eqs. (10), (12b) and (14) when compound are treated as non-association (NA) or as association with a two-site scheme (2B). Absolute average deviations (AAD) of vapour pressures P^σ and molar densities $\rho_{\text{liq.}}$

Table 5. Solubilities absolute average deviations (AAD(x_2)) when CPA Eos is used with $k_{ij} = 0$ (prediction) for HFC-IL systems when compound is treated as non-association (NA) or as association with a two-site scheme (2B).

Table 6. Calculated mean values of RTIL solubility parameters δ_1.

Table 7. Values for the parameters D and E of Eq. 18 and total solubility average deviation (AAD(x_2)) for each HFC.

Table 8. Values for A/R of Eq. 22 for HFC-RTIL systems and solubility absolute average deviation (AAD(x_2)) of each HFC data set.

Table 1. Compounds used in this work.

Name	Abbreviation	Chemical Structure	Origin	Fraction Purity
1-ethyl-3-methylimidazolium bis(trifluoromethanesulfonyl)amide	$[C_2mim][NTf_2]$	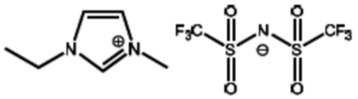	Io – li – tec	>0.98 (mass)
Trihexyltetradecylphosphonium bis(trifluoromethylsulfonyl)imide	$[P_{6,6,6,14}][NTf_2]$	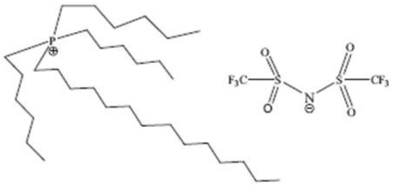	*CYTEC*	>0.98 (mass)
N-methyl-2-hydroxy ethylammonium propionate	[m-2-HEA][Pr]	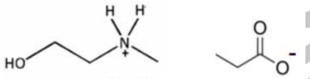	Synthesized [a]	—
N-methyl-2-hydroxy ethylammoniumpentanoate	[m-2-HEA][P]	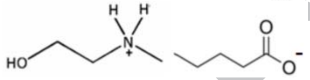	Synthesized [a]	—
Fluoromethane	CH_3F	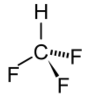	Gas UK Limited	0.990 (moles)
Difluoromethane	CH_2F_2	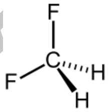	Gas UK Limited	0.990 (moles)
Trifluoromethane	CHF_3	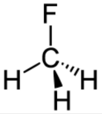	Gas UK Limited	0.990 (moles)

[a] Supplied by Prof João A.P. Coutinho from Aveiro University, Portugal. The details about the synthesis can be found in [58].

Table 2.HFC solubility parameters δ_2 at the boiling point temperature. Values retrieved from [59].

Solute	$\delta_2 /(\text{J}\cdot\text{cm}^{-3})^{1/2}$
CHF_3	17.651
CH_2F_2	20.627
CH_3F	20.373

Table 3. Experimental solubilities x_2 and Henry's constants H_{21} for CHF_3, CH_2F_2 and CH_3F in RTILs at o.101 MPa as a function of temperature.

Solvent	T/K [a]	$10^4 \cdot x_2$ [b]	H_{21}/MPa [c]	T/K [a]	$10^4 \cdot x_2$ [b]	H_{21}/MPa [c]	T/K [a]	$10^4 \cdot x_2$ [b]	H_{21}/MPa [c]
		CHF_3			CH_2F_2			CH_3F	
$[C_2mim][NTf_2]$									
	288.13	362.7	2.752	288.11	1135	0.893	288.15	571.4	1.822
	293.23	350.1	3.018	293.56	984.4	1.023	293.43	486.3	2.112
	298.16	298.6	3.290	298.33	902.5	1.125	298.19	462.4	2.249
	303.17	278.1	3.669	303.27	798.2	1.293	303.17	401.5	2.503
	308.17	254.2	4.035	308.19	715.0	1.444	308.19	398.8	2.677
$[P_{6,6,6,14}][NTf_2]$									
	288.15	588.6	1.635	288.15	1330	0.774	288.15	909.2	1.123
	293.15	571.7	1.736	293.21	1235	0.836	293.15	814.0	1.218
	298.15	518.4	1.912	298.35	1190	0.886	298.36	767.6	1.292
	303.19	462.3	2.129	303.19	1058	0.959	303.15	748.6	1.360
	308.39	436.0	2.316	308.23	1004	1.010	308.15	665.3	1.479
[m-2-HEA][Pr]									
	288.15	144.4	6.945	288.15	362.4	2.789	288.15	154.2	6.418
	293.21	129.4	7.783	293.21	314.0	3.175	293.27	141.2	7.160
	298.17	115.6	8.585	298.17	280.6	3.669	298.17	129.7	7.988
	303.27	107.2	9.155	303.27	245.4	4.030	303.19	121.0	8.448
	308.23	103.5	9.906	308.23	243.5	4.292	308.23	109.5	9.267
[m-2-HEA][P]									
	288.15	204.0	4.901	288.15	468.4	2.240	288.15	215.3	4.715
	293.15	192.4	5.440	293.15	400.0	2.533	293.17	202.1	5.104
	298.73	181.6	5.665	298.15	376.1	2.706	298.45	184.3	5.393
	303.15	162.7	6.129	303.32	331.7	3.109	303.17	174.8	5.797
	308.36	154.9	6.758	308.21	305.5	3.426	308.17	167.8	6.002

[a] $\delta T = 0.01\,\text{K}$. [b] Calculated from Eqs. (1) to (5). Estimated standard error of 0.1 %. [c] $\delta H_{21} = 10\,\text{Pa}$.

Table 4. Pure component CPA parameters a_0, c_1, b and β Eqs. (10), (12b) and (14) when compounds are treated as non-association (NA) or as association with a two-side scheme (2B). Absolute average deviations (AAD) of vapour pressures P^σ and molar densities $\rho_{\text{liq.}}$

Compound	a_0 /(Pa·m^6·mol^2)	c_1	$10^5 \cdot b$ /(m^3·mol^{-1})	ε /(J·mol^{-1})	$10^4 \cdot \beta$	$0.01 \cdot \mathrm{AAD}(x)$ [a]	
						P^σ	$\rho_{\text{liq.}}$
			NA				
[C_2mim][NTf_2]	25.12	0.58	29.50			2.3	1.1
[$P_{6,6,6,14}$][NTf_2]	35.96	1.11	71.41				1.0
[m-2-HEA][Pr]	4.53	2.08	13.12				0.5
[m-2-HEA][P]	4.88	2.31	16.80				0.5
CHF_3	0.50	0.78	3.83			0.1	0.5
CH_2F_2	0.54	0.74	3.46			0.3	0.9
CH_3F	0.44	0.64	3.12			0.6	0.6
			2B				
[C_2mim][NTf_2]	25.79	0.36	29.80	25400	1.87	2.4	1.6
[$P_{6,6,6,14}$][NTf_2]	35.14	1.09	71.10	13220	1.00		1.2
[m-2-HEA][Pr]	5.90	1.22	12.78	27124	1.27		2.9
[m-2-HEA][P]	6.81	1.31	16.22	27675	1.19		3.8

[a] $0.01 \cdot \mathrm{AAD}(x) = (1/N_p)\sum_{i=1}^{N_p}\left|x_{\text{calc},i} - x_{\text{exp},i}\right| / (x_{\text{exp},i})$. Here x either P^σ or ρ_{liq}.

Table 5. Solubility absolute average deviations (AAD(x_2)) when CPA Eos is used with $k_{ij} = 0$ (prediction) for HFC-IL systems when compound is treated as non-association (NA) or as association with a two-site scheme (2B).

$0.01 \cdot \mathrm{AAD}(x_2)^a$		[C_2mim][NTf_2]	[$P_{6,6,6,14}$][NTf_2]	[m-2-HEA][Pr]	[m-2-HEA][P]	Mean
CHF_3	CPA(NA)	49	35	62	44	48
	CPA(2B)	49	27	65	37	45
CH_2F_2	CPA(NA)	36	52	3	25	29
	CPA(2B)	36	46	11	6	25
CH_3F	CPA(NA)	31	54	4	7	24
	CPA(2B)	37	54	16	7	29

[a] $0.01 \cdot \mathrm{AAD}(x_2) = (1/N_p)\sum_{i=1}^{N_p}\left|x_{2,\mathrm{calc}} - x_{2,\mathrm{exp}}\right| / (x_{2,\mathrm{exp}})$.

Table 6. Calculated mean values of RTIL solubility parameters δ_1.

Solvent	$/ (\mathrm{J} \cdot \mathrm{cm}^{-3})^{1/2}$
$[C_2mim][NTf_2]$	38.3
$[P_{6,6,6,14}][NTf_2]$	19.4
[m-2-HEA][Pr]	57.2
[m-2-HEA][P]	49.3

Table 7. Values for the parameters D and E of Eq. 18 and total solubility average deviation (AAD(x_2)) for each HFC.

Solute	D	E /([cm^3/J]$^{1/2}$· K)	$0.01 \cdot$ AAD(x_2) [a]
CHF_3	14.38	0.2676	25.2
CH_2F_2	13.53	0.3056	31.5
CH_3F	14.01	0.3851	26.3

[a] $0.01 \cdot \mathrm{AAD}(x_2) = (1/N_p)\sum_{i=1}^{N_p}\left|x_{2,\mathrm{calc}} - x_{2,\mathrm{exp}}\right| / (x_{2,\mathrm{exp}})$.

Table 8. Values for A/R of Eq. 22 for HFC-RTIL systems and solubility absolute average deviation (AAD(x $_2$)) of each HFC data set.

(A/R)/K	[C_2mim][NTf_2]	[$P_{6,6,6,14}$][NTf_2]	[m-2-HEA][Pr]	[m-2-HEA][P]	$0.01 \cdot \mathrm{AAD}(x_2)$ [a]
CHF_3	-2203.99	-1165.48	-1634.02	-2262.90	3.4
CH_2F_2	-1527.60	-1733.34	-1952.48	-3657.15	5.9
CH_3F	-1939.93	-861.730	-1367.65	-2968.58	5.8

[a] $0.01 \cdot \mathrm{AAD}(x_2) = (1/N_p)\sum_{i=1}^{N_p}\left|x_{2,\mathrm{calc}} - x_{2,\mathrm{exp}}\right| / (x_{2,\mathrm{exp}})$.

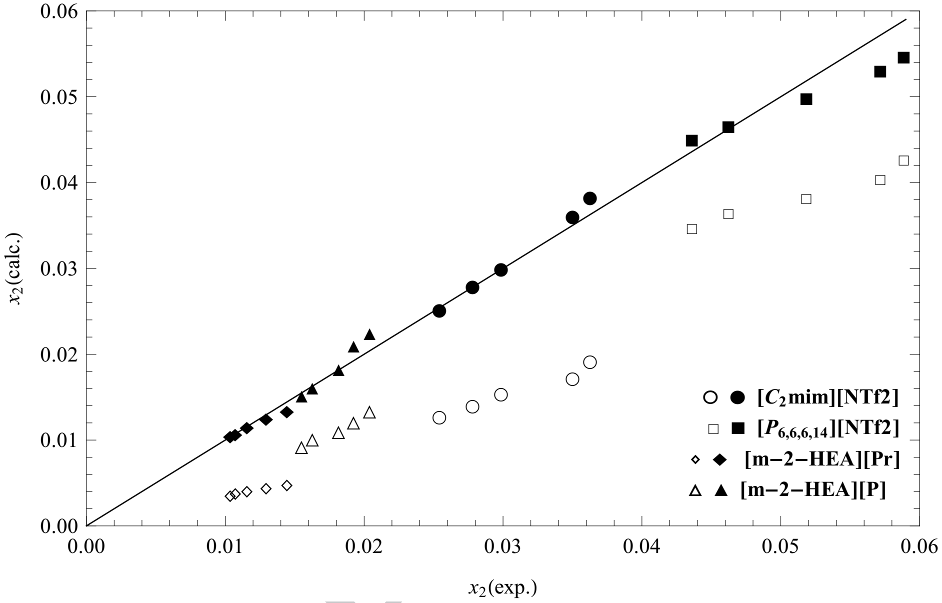
0.06
0.05
0.04
0.03
0.02
0.01
0.00
x_2(calc.)
0.00
0.01
0.02
0.03
0.04
0.05
0.06
x_2(exp.)
○ ● $[C_2$mim][NTf2]
□ ■ $[P_{6,6,6,14}]$[NTf2]
◇ ◆ [m−2−HEA][Pr]
△ ▲ [m−2−HEA][P]

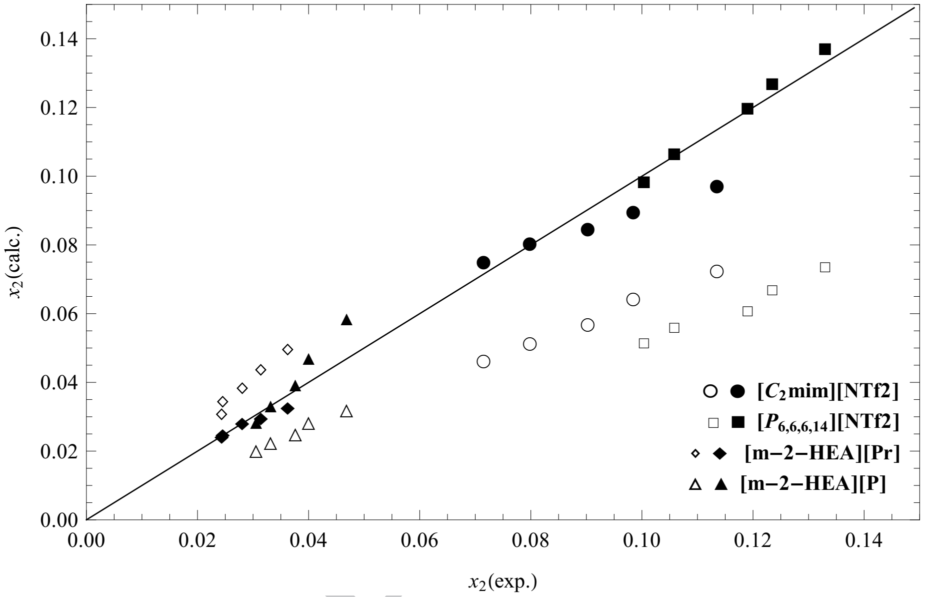

0.00
0.02
0.04
0.06
0.08
0.10
0.12
0.14
x_2(calc.)
x_2(exp.)
○ ● [C_2mim][NTf2]
□ ■ [$P_{6,6,6,14}$][NTf2]
◇ ◆ [m−2−HEA][Pr]
△ ▲ [m−2−HEA][P]

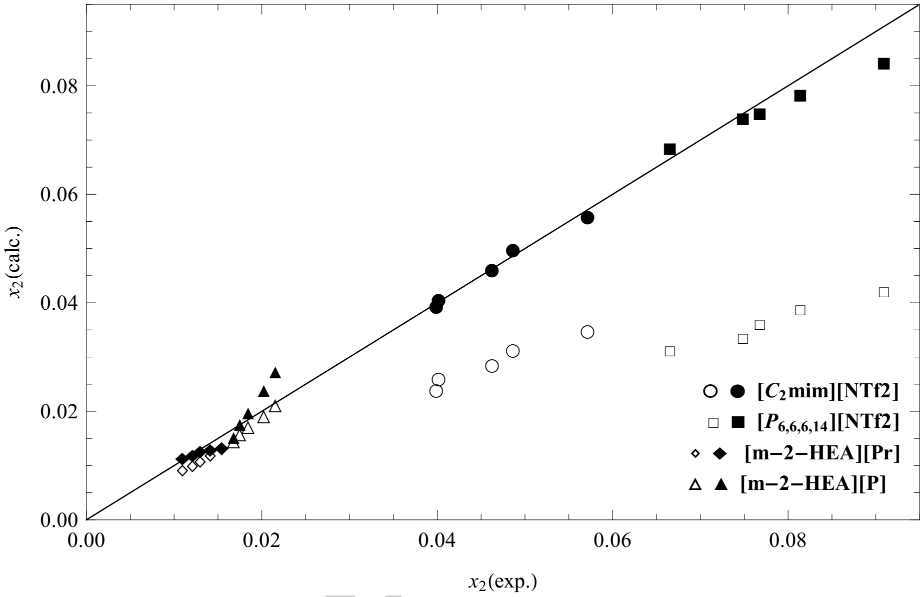
0.00
0.02
0.04
0.06
0.08
0.00
0.02
0.04
0.06
0.08
x_2(calc.)
x_2(exp.)
○ ● [C_2mim][NTf2]
□ ■ [$P_{6,6,6,14}$][NTf2]
◇ ◆ [m−2−HEA][Pr]
△ ▲ [m−2−HEA][P]

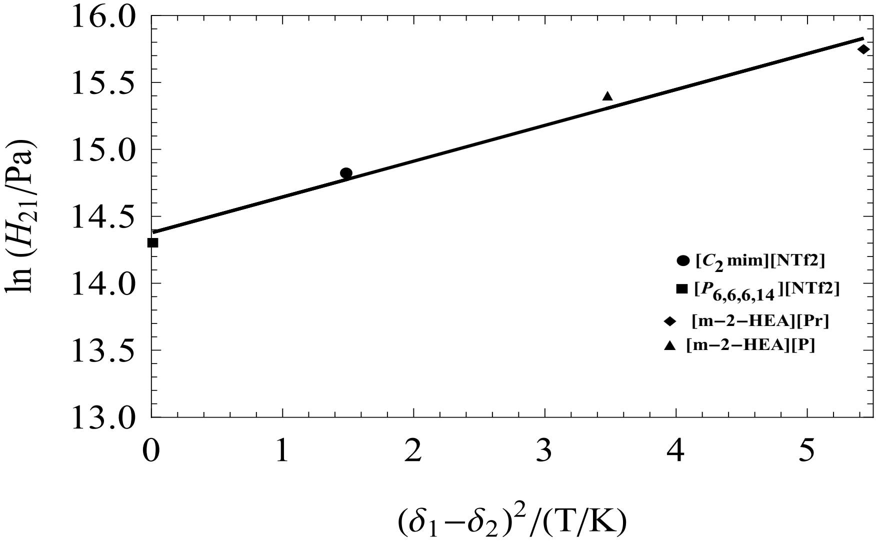
16.0
15.5
15.0
14.5
14.0
13.5
13.0
ln (H_{21}/Pa)
0
1
2
3
4
5
($\delta_1-\delta_2$)^2/(T/K)
● [C_2 mim][NTf2]
■ [$P_{6,6,6,14}$][NTf2]
◆ [m−2−HEA][Pr]
▲ [m−2−HEA][P]

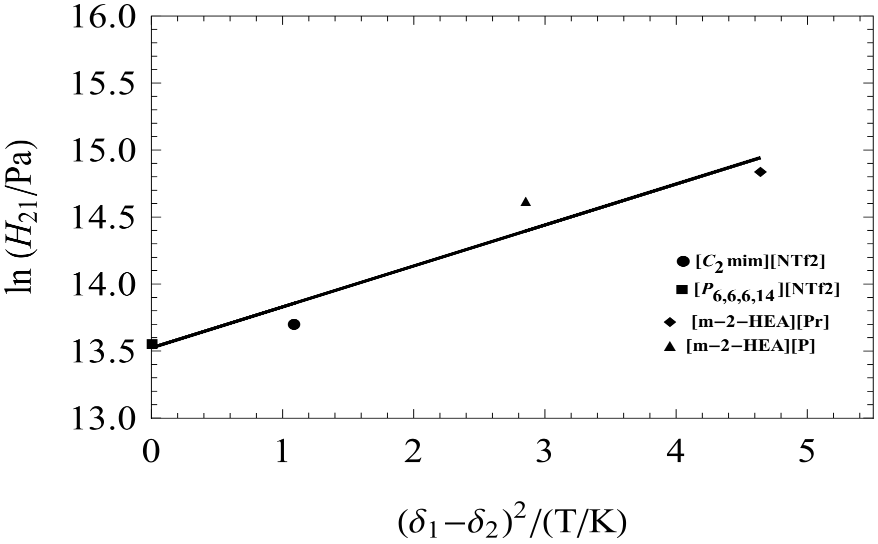
16.0
15.5
15.0
14.5
14.0
13.5
13.0
ln (H_{21}/Pa)
0
1
2
3
4
5
$(\delta_1-\delta_2)^2$/(T/K)
● [C_2 mim][NTf2]
■ [$P_{6,6,6,14}$][NTf2]
◆ [m−2−HEA][Pr]
▲ [m−2−HEA][P]

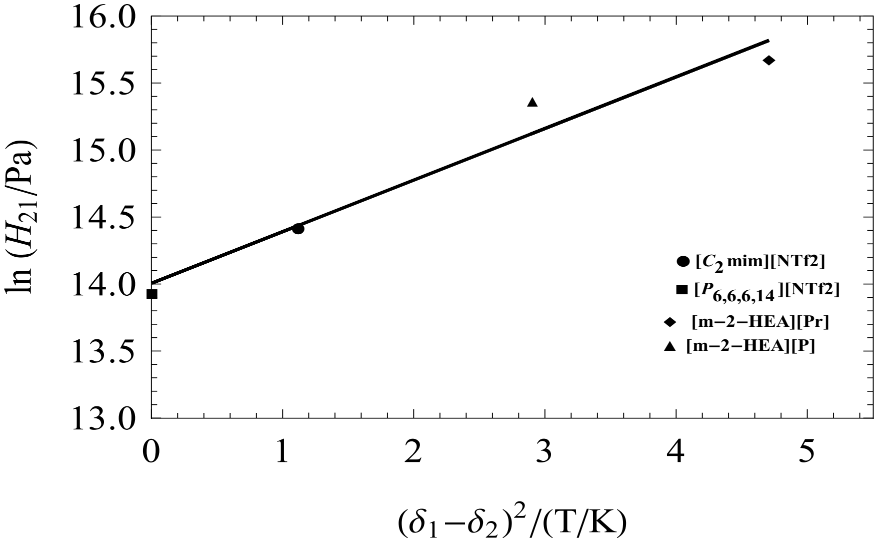
16.0
15.5
15.0
14.5
14.0
13.5
13.0
0
1
2
3
4
5
$\ln (H_{21}/\text{Pa})$
$(\delta_1-\delta_2)^2/(\text{T/K})$
● $[C_2\,\text{mim}]$[NTf2]
■ $[P_{6,6,6,14}]$[NTf2]
◆ [m−2−HEA][Pr]
▲ [m−2−HEA][P]

Experimental data on the gas solubility of CHF_3, CH_2F_2 and CH_3F in room-temperature ionic liquids (RTILs) at 1atm is reported;

CPA EoS is applied to model the solubilities of HFCs in RTILs with a good qualitative agreement;

Semi-empirical model based on the regular-solution theory is correlated to experimental data with AAD (x_2) values around 5%;

HFCs are more soluble in [C_2mim][NTf_2] and [$P_{6,6,6,14}$][NTf_2] up to 2.5 times more than in ammonium-based RTILs;